Published in final edited form as:
Int J Geriatr Psychiatry. 2013 September ; 28(9): 959–970. doi:10.1002/gps.3911.

MORPHOMETRIC ANALYSIS OF VASCULAR PATHOLOGY IN THE ORBITOFRONTAL CORTEX OF ELDERLY SUBJECTS WITH MAJOR DEPRESSION

Jose Javier Miguel-Hidalgo, Ph.D., D.M.Sc.[1], **Wei Jiang, M.D.**[2], **Lisa Konick, Ph.D.**[3], **James C. Overholser, Ph.D.**[4], **George J. Jurjus, M.D.**[3,5], **Craig A. Stockmeier, Ph.D.**[1,3], **David Steffens, M.D.**[2], **K. Ranga R. Krishnan, M.D.**[2], and **Grazyna Rajkowska, Ph.D.**[1]

[1]Psychiatry and Human Behavior, University of Mississippi Medical Center, Jackson, MS

[2]Psychiatry and Behavioral Sciences, Duke University Medical Center, Durham, NC

[3]Psychiatry, Case Western Reserve University, Cleveland, OH

[4]Psychology, Case Western Reserve University, Cleveland, OH

[5]Department of Psychiatry, Cleveland VA Medical Center, Cleveland, OH

Abstract

Objective—Late-life depression has been associated with risk for cerebrovascular pathology, as demonstrated in neuroimaging studies of older depressed patients, as well as mood disorder following cerebrovascular accidents. However, more research is needed on neuroanatomical changes in late-life depression, where there has been no clearly documented link to brain injury. Such studies should examine morphological changes in medium and small sized vessels that supply the cortical gray and white matter.

Methods—The present study used a non-specific histological Nissl staining and a more vessel-specific immunolabeling with endothelial marker von Willebrand Factor (vWF) to estimate density and size of blood vessel segments in the orbitofrontal cortex of 16 elderly subjects with major depressive disorder (MDD) and 9 non-psychiatric comparison subjects.

Results—The density of Nissl-stained vessel segments and of segments with perivascular spaces was higher in subjects with MDD than in comparison subjects in gray (GM) and white matter (WM). In GM, the density of vWF-immunoreactive segments with cross-sectional areas greater than 800 μm^2 was higher in MDD. In WM, only the density of vWF-immunoreactive segments with patent perivascular spaces and diameters larger than 60 μm was higher in subjects with MDD. Also in the WM, only subjects with late-onset MDD presented a significantly higher density of vWF-positive segments than comparison subjects.

Conclusions—In elderly subjects with MDD, there appear to be morphological changes that increase visibility of medium-sized vessel segments with some labeling techniques, and this increased visibility may be related to increased patency of perivascular spaces around arterioles.

Corresponding author: Jose Javier Miguel-Hidalgo, Department of Psychiatry and Human Behavior, University of Mississippi Medical Center, 2500 N. State St., Box 127, Jackson, MS 39216-4505, Phone: (601)984-5791, Fax: (601)984-5899, jmiguel-hidalgo@umc.edu.

Conflicts of interest
The authors declare no conflicts of interest.

Keywords

Depression; prefrontal cortex; blood vessels; morphometry

INTRODUCTION

Clinical studies associate late-life depression with risk factors for cerebrovascular disease (Krishnan, 2000; Lesperance et al., 2004). Epidemiological studies report that older patients with hypertension, diabetes, or heart disease are at higher risk for depression (Taylor and Krishnan, 2003). Moreover, magnetic resonance imaging (MRI) studies have indicated that white matter (WM) lesions (hyperintensities) are more common in elderly MDD subjects than in non-psychiatric subjects of comparable age (Taylor et al., 2003b), particularly in patients with late-onset depression (Figiel et al., 1991; Krishnan et al., 1988; Coffey et al., 1989; Coffey et al., 1990).

Among older depressives hyperintensities are prevalent in orbitofrontal cortex (OFC) WM, internal capsule, periventricular regions and in basal ganglia (Greenwald et al., 1998; MacFall et al., 2001; Taylor et al., 2001; Coffey et al., 1989; Coffey et al., 1990; Kumar and Miller, 1997; Steffens and Krishnan, 1998; Steffens et al., 1999; Krishnan et al., 2004). An association between smaller OFC volume and increased hyperintensities in basal ganglia was noted in elderly depressed patients (Lee et al., 2003). Thus, the available evidence led to hypothesize that WM lesions disrupt axonal tracts and cause neuronal pathology in the gray matter (GM) of elderly MDD subjects (Lee et al., 2003; Taylor et al., 2001; Alexopoulos et al., 1997). A postmortem cell-counting study revealed a 14% reduction in the density of neurons in the OFC of elderly MDD subjects (Rajkowska et al., 2005), especially in cortical layers III and V, which contain pyramidal neurons. The authors suggest that degeneration of these neurons, with axons running in the WM, is related to hyperintensities observed in the OFC. Functional disruption in the OFC might be of great relevance to affective disorders in the elderly because this brain region is highly involved in emotional regulation and decision-making processes (Grafman *et al.*, 1996; MacFall *et al.*, 2001; Erickson *et al.*, 2005; Savitz *et al.*, 2007). In addition, neuroimaging studies have shown reduced volume and abnormal brain activation of the OFC in midlife and elderly depressed patients (Vaishnavi and Taylor, 2006; Lesser *et al.*, 1994; Brassen *et al.*, 2008; Lai *et al.*, 2000; Lee *et al.*, 2003; Taylor and Krishnan, 2003).

Histopathological studies (Thomas et al., 2002a; Thomas et al., 2002b; Munoz et al., 1993) suggest that prefrontal hyperintensities in MDD correspond to cerebrovascular lesions of ischemic appearance (Taylor et al., 2001). Thus, the increased frequency of these lesions in the elderly has led to proposing the existence of late-life vascular depression (Alexopoulos, 2006; Camus et al., 2004). However, in the histopathological studies above only WM from dorsolateral prefrontal cortex was examined. Moreover, the authors focused on correlating MRI-detected large WM lesions with their morphology in histological sections, but did not examine in detail morphological alterations in the numbers or density of medium-sized and small blood vessels. In fact, hyperintensities and vascular lesions are also frequent in psychiatrically normal subjects and in psychiatric disorders other than depression. Thus, vascular changes in the pathophysiology of depression might not be just a mediator of hyperintensities-related processes, but could be contributing independently to defective neurotransmission in the prefrontal cortex. Medium and small-sized vessels are surrounded by astrocyte endfeet and both astrocytes and neurons strongly interact with vessels during neuronal activation, raising the possibility that morphological alterations of these vessels in relevant areas such as the OFC contribute to the pathophysiology of depression. Therefore, the present study aimed to determine whether the morphology of medium-sized and small

vessels is altered in depression by estimating the density and size of blood vessel profiles and their perivascular spaces in GM and WM of the rostral OFC of elderly patients with either early- or late-onset MDD, as compared to non-psychiatric subjects.

METHODS

Subjects

Postmortem brain tissue was obtained from 25 elderly subjects (average age: 70; range: 54–86 years old) (Table 1 and Supplemental table 1) Tissue originated from autopsies at the Cuyahoga County Coroner's Office, Cleveland, OH. The protocol for the collection of brain samples was approved by the Institutional Review Boards at the University of Mississippi Medical Center and the University Hospitals of Cleveland. Informed written consent was obtained from next-of-kin for all subjects. Subjects were assigned to two groups based on a retrospective psychiatric assessment as described (Rajkowska et al., 2005): 1) Sixteen subjects with major depressive disorder (MDD), and 2) Nine psychiatrically normal comparison subjects. The MDD subjects met DSM-IV (American Psychiatric Association, 1994) criteria for an Axis I diagnosis of MDD; 15 subjects met clinical criteria for MDD within the final month of life, while one subject was in full remission. Medical history of hypertension and/or cardiovascular insufficiency in MDD subjects was determined according to: 1) postmortem pathological examination, 2) doctor or hospital records, and 3) reports obtained by the interviewer with the family. The comparison subjects were similar in age, gender, race and postmortem delay to the MDD group. The comparison group was free of Axis I psychopathology or neurological disorders, and all subjects had a history of hypertension and/or cardiovascular insufficiency. Subjects were excluded if there was any evidence of Alzheimer's disease, other forms of non-Alzheimer dementia or stroke. Summary details of the evaluation of medical and autopsy records for cardiovascular and cerebrovascular gross pathology by a cardiologist (W. J.) are presented in Supplemental file 1.

Eleven MDD subjects had late-onset depression (>50 years of age), whereas five subjects early-onset depression (between 20–30 years of age). Of the MDD subjects, nine died of suicide. Fourteen MDD subjects were ever treated with antidepressant drugs and 11 had antidepressant drugs prescribed within the last month of life (see Table 1, and supplemental data table 1). Brain weight at autopsy was not different between comparison subjects and subjects with MDD (1,319.11±115.20 grams and 1,294.19±132.49 grams, respectively, T-test $t=-0.472$, $p=0.641$)

Tissue

Blocks of postmortem brain tissue from the frontal lobe were fixed in 10% formalin and embedded in 12% celloidin (Rajkowska and Goldman-Rakic, 1995; Rajkowska et al., 1999). Sections cut at a thickness of 40 μm were stained with cresyl violet (Nissl staining). Cresyl violet stains rough endoplasmic reticulum and free polyribosomes in neurons, glia and endothelial cells. Cytoarchitectonic criteria were used to sample three sections evenly spaced by 800 μm from the rostral OFC corresponding to Brodmann's area 47 (Uylings et al., 2010). These were the same sections used for cell counting in our previous studies (Rajkowska et al., 1999; Rajkowska et al., 2005). Nissl-type stains allow for unequivocal detection only of relatively large blood vessels while small vessels are difficult to visualize. To analyze the entire population of blood vessels and capillaries, three additional sections immediately adjacent to the Nissl-stained sections were immunostained for von Willebrand factor (vWF, this protein binds coagulation factor VIII), a specific marker of endothelial cells using specific antibodies (rabbit anti-vWF, Sigma, cat. no. F3502; dilution 1:1000). Celloidin removal and immunohistochemistry proceeded according to published protocols

(Miguel-Hidalgo and Rajkowska, 1999). Sections were mounted on slides and coverslipped. Thickness of immunostained sections shrunk from 40 μm to approximately 17–18 μm.

1) Morphometric analysis of Nissl-stained blood vessels—The density and size of blood vessels was measured in GM and underlying WM of ORB. The density (blood vessel profiles per 1 mm^3 of tissue) was estimated by using a direct three-dimensional counting method inspired by the optical dissector principle in three histological sections per brain, considering the isolated vessel segment as the counting unit. The counting technique was not strictly stereological because vessels are not discrete structures within the section as required for actual stereological counts. Moreover, vessels are continuous and thus the vessel segments resulting from histological sectioning extend across both surfaces of the section. Three-dimensional counting served only to ensure that vessels cut across the surfaces of the section. Thus, we only counted segments of vessels as projected onto the two-dimensional visual field of the microscope, even if we present their density referred to the volume of tissue (the dimensions of the counting frames were 556X392X40 μm). This density was measured in a series of counting frames that spanned the entire gray matter and 2 frames of underlying white matter using a 20X microscope objective (Fig. 1). In addition, the size of the perivascular widening (i.e., unstained spaces surrounding vessels) was estimated by the area of the segment itself (D1) and the area enclosed by the outer lining of the perivascular space (D2), and subtracting D1 from D2. (Fig. 2).

2) Morphometric analysis of vWF-immunoreactive vessel segments in GM and the underlying WM—Morphometric parameters of vWF-immunoreactive (vWF-IR) segments were estimated using ImageJ analysis software (version 1.4, National Institutes of Health) in three sections per subject. A frame with a width of 685 μm containing all cortical layers was defined in area 47 for GM while a frame of the same width and height (685 μm) was defined for the underlying WM (Fig. 3A). vWF immunostaining of vessel segments was distinguishable from the non-specific background staining (Fig. 3A, top right inset). Thresholding was implemented with 20 gray levels of optical density over the background level (gray levels were from 0 to 255) and the area of vessel segments measured. ImageJ software was then used to generate ellipses for each vessel profile calculated from the area of the profile and the linear dimensions of the longest and shortest axes of the profile. The dimension of the short axis of the ellipse was taken as an estimate of vessel diameter (Fig. 3B). Thus, four sample estimates were first calculated: 1) areal fraction of all immunoreactive profiles in one frame; 2) average area of the individual profiles; 3) average diameter of individual profiles; and 4) packing density of profiles.

In addition, we analyzed the packing density of vessel segments sorted into different classes based upon the area and the diameter of individual profiles. Five area-based (a) size-classes of vessel segments were distinguished: $a<200$, $200\leq a<400$, $400\leq a<600$, $600\leq a<800$, $a\geq 800$ μm^2. Four diameter-based (d) classes were distinguished using the mean (m) and standard deviation (s) of the diameters of all measured segments as cut-off values: $d<(m-s)$, $(m-s)\leq d<m$, $m\leq d<(m+s)$, $d\geq m+s$. The criteria to define the size classes sought to be systematic, that is, to define classes based on an objective rule that did not favor an a priori definition of a particular class within the range of sizes found in the tissue. Thus, we defined the area classes with one class every 200 μm^2, and for diameter we used the standard deviation of the mean diameter of the controls to set the distance between classes with the mean as the central value. That is, each class was separated from the other by one standard deviation. Although other classifications by a systematic rule are possible, the fact that diameter and area classes obeyed two different rules increased the probability of finding morphological changes if they genuinely existed.

3) Morphometric analysis of large vWF-IR vessels in deep WM—The density of vessel segments in WM is significantly lower and the diameter of these profiles is larger on average than in GM. Many segments larger than 60 μm in diameter were surrounded by perivascular spaces between the immunolabeled endothelium and the brain parenchyma. The packing density of all immunoreactive vessel segments with diameter >60 μm and the density of vessels with observable perivascular spaces was estimated in the WM of OFC (Fig. 2) using Stereo Investigator software (version 8.0, Microbrightfield, Inc.) by an operator naïve to the diagnoses. The density of these vessel segments, their area as projected onto the visual field and the size of perivascular spaces was measured with ImageJ software.

STATISTICAL ANALYSIS

Influences of age, postmortem delay, storage time of tissue in formalin, storage time of celloidin sections in ethanol, brain tissue pH, duration of illness and onset of illness on the various parameters studied were also examined by Pearson correlation analyses. There was no significant difference in age or time in formalin between MDD and comparison subjects (ANOVA), but there was a trend for a difference in pH and storage time of sections in ethanol. Thus, the averages for each of the sample estimates obtained in the three sections per brain were subjected to a single factor (disease) analysis of covariance (ANCOVA) between the depressed and comparison groups using brain pH and storage time in ethanol as covariates. ANCOVA was also performed for the packing density of each of the size classes of immunoreactive profiles. One of the subjects with MDD could only be used for immunohistochemical staining and another one only for Nissl staining. Thus, the statistical analyses for each staining procedure includes 15 MDD and 9 comparison subjects. Numerical data are presented as mean±standard deviation.

RESULTS

1. Analysis of Nissl-stained vessels in the OFC

In Nissl-stained material ANCOVA revealed significantly higher density of identifiable blood vessel segments in the GM of MDD subjects than in comparison subjects (Fig. 4A) ($F(1, 20) = 36.60$, $p< 0.0001$; MDD: 380.6±120.1 segments/mm^3, comparison: 97.31±50.5 segments/mm^3). Likewise, there was significantly higher density of identifiable vessels in the WM in MDD subjects (Fig. 4B) (ANCOVA $F(1,20) = 26.53$, $p< 0.0001$; MDD: 312.9±126.8 segments/mm^3, comparison: 81.8±39.4 segments/mm^3). To ascertain possible changes in average size of vessel segments, every observed profile was outlined size determined by averaging the equivalent diameter (calculated by finding the diameter of the circle with the same area as the segment). The diameter of segments in MDD subjects was not significantly larger than in comparison subjects (81.96±53.63 vs. 63.40±30.33 μm, respectively, ANCOVA $F(1, 20)=0.82$, $p=0.38$) (Fig. 4C). The area of vessels was not significantly different either (2156.95±1533.05 vs. 1143.55±441.03 μm^2, ANCOVA $F(1, 20)=2.32$, $p=0.14$). In addition, we outlined the perivascular spaces surrounding some vessels segments, because individual differences were observed in the prevalence of these spaces. The average area of the perivascular space in MDD subjects was not significantly larger than that in comparison subjects (area 4346.18±2128.54 vs. 2754.08±1485.96 μm^2, respectively, ANCOVA $F(1,20)=1.85$, $p=0.19$; diameter 32.25±12.02 vs 22.45±5.99 μm, respectively, ANCOVA $F(1,20)=2.59$, $p=0.12$) (Fig. 4D).

2. Analysis of vWF-IR vessels in the GM and adjacent WM of the OFC

The density and area fraction of vessel segments and were significantly greater in GM than in WM in all subjects (Fig. 3). In contrast, the diameter of vWF-IR vessel segments was significantly larger in WM than in GM.

There was no significant difference in the packing density or area fraction of all vWF-IR vessel segments between comparison and MDD subjects in either WM or in GM (Table 2, supplemental material). Average area and average diameter of vWF-IR vessel segments in GM and WM were not significantly different between groups either (see Table 3, supplemental material).

Since the diameters of vessel segments varied, segments were further subdivided according to the size of their sectional areas and the packing density of each size class was compared between groups (see Methods section earlier). In GM the packing density of segments larger than 800 μm2 was significantly higher in the MDD group than in the comparison group (MDD: 3.01±1.81, comparison: 2.36±1.82 segments/mm^2, ANCOVA, $F(1,20)=4.324$, $p<0.05$), but there was no difference for profiles smaller than 800 μm^2 (Fig. 5).

Our analysis of vWF-IR segments included GM and WM. The majority of these segments correspond to capillaries and other small vessels. In histological sections throughout the cortex, only a few segments with diameters larger than 50 μm stand out among a majority of small and medium-sized vessels. Relatively large vessels in the WM may play a role in lesions present in patients with late-onset vascular depression (Thomas et al., 2002b). Accordingly, a separate size analysis of large vWF-IR vessels in WM is presented in the next paragraph.

3. Analysis of large vWF-IR vessels in the deep WM of OFC

The density of large vessel segments (>60 μm in diameter) with perivascular spaces was significantly higher in MDD than in the comparison group (MDD: 0.88±0.28, comparison: 0.57±0.19 segments/mm^2, ANCOVA $F(1, 20)= 8.12$ $p=0.01$). However, there was no significant difference in the density of all large vWF-IR vessels between groups (MDD: 1.06±0.35, comparison: 0.89±0.30 segments/mm^2, ANCOVA $F(1, 20)=2.99$ $p=0.10$).

4. Morphometry of large vessel segments of the OFC in EARLY versus LATE onset MDD

MDD subjects were divided into early onset (<50 years of age) and late onset (>50 years of age) depression subgroups. There was a significant difference between comparison subjects and both MDD subgroups in density of Nissl-stained vessel segments in GM and WM (ANCOVA $F(2,19)=17.39$, $p < 0.001$ and ($F(2,19)=12.63$, $p < 0.001$ respectively), and in density of large vWF-IR vessels (diameter > 60 μm) with perivascular spaces in WM (ANCOVA $F(2,19)=6.92$, $p = 0.005$) (Fig. 6), but no difference between early and late onset subjects. The density of large vWF–IR vessel segments with perivascular spaces in WM was significantly higher in late-onset MDD subjects (Bonferroni, $p = 0.005$), but early onset MDD subjects were not significantly different from comparison subjects (Bonferroni, $p = 0.382$) (Fig. 6). In the group of MDD subjects, there was no significant difference between subjects dying by suicide and those dying by other causes either in the morphological variables based on Nissl staining or those based on immunohistochemistry for vWF.

DISCUSSION

The present study found that the density of Nissl-stained vessel segments and segments with perivascular spaces was higher in MDD subjects than in comparison subjects in GM and WM. However, with vessel specific immunostaining for vWF only segments with cross-sectional areas greater than 800 μm2 were higher in the GM of subjects with MDD. In WM, only the density of segments with perivascular spaces and diameters larger than 60 μm were higher in subjects with MDD. Also in the WM, only subjects with late-onset MDD were significantly different from comparison subjects in the density of vWF-IR segments.

Previous studies focused on the possibility of vascular pathology in depression, although those studies sought to determine the gross morphology of WM hyperintensities and associated blood vessels (Thomas et al., 2001; Thomas et al., 2002b; Thomas et al., 2003). In line with this research, Thomas et al. (29) used semiquantitative grading scores to determine the degree of vessel pathology in subjects with late-life depression. Thomas and collaborators (Thomas et al., 2002a; Thomas et al., 2000) also reported on the extent of blood vessels immunoreactive for the inflammation-associated protein ICAM-1 in late-life depression. In contrast to those studies, the present investigation used 2- and 3-dimensional microscopic measurements to quantify morphometric parameters of all vessel segments detectable within GM and WM.

It could be argued that in Nissl-stained sections the smallest capillaries and veins were missed (or confused with glial cell nuclei), and thus the survey of vessels was biased in favor of larger vessels. Nevertheless, since the researchers were blind to diagnosis, this bias would apply to both MDD and comparison subjects. Accordingly, in MDD subjects, Nissl-stained vessels may have been more visible due to any of these reasons: 1) larger segments were actually more abundant in MDD subjects, and 2) large segments were more easily identified, and thus counted more frequently in MDD. Visibility could have been enhanced by perivascular spaces or thickened walls around larger vessels. Because these possible explanations for visibility changes with Nissl-staining depend on morphological changes of vessel walls and their interaction with the neuropil, additional analyses with specific molecular markers will be needed to determine the cause of increased visibility of large vessels in MDD.

In contrast, it should be noted that the average density of vWF-IR vessel profiles in sections neighboring the Nissl-stained sections was not changed in MDD. This apparent discrepancy with Nissl-staining suggests that some small vessels (revealed by vWF-immunostaining) might not have been as visible in Nissl-stained material in comparison subjects as in MDD subjects. Lack of visibility in comparison subjects may be due to vessels being firmly attached to the neuropil and not showing pathological features. This attachment would make it difficult to distinguish the smallest vessels in Nissl preparations, but not in vWF immunostaining where only endothelial cells, but not neurons or glial cells, are stained. Additionally, in subjects with MDD there may be increased density of arterioles, medium-sized and larger vessels. Therefore, there may be a significantly higher density of vWF-IR vessels with cross-sectional areas over 800 μm^2 in MDD subjects than in non-psychiatric subjects. Such an explanation, together with data presented here reporting no differences in overall density of vWF-IR segments of less than 800 μm^2, would also be consistent with the absence of small vessel pathology in late-life MDD when using semi-quantitative measurements (Thomas et al., 2001).

Morphological data reported in the present study suggest subtle vascular pathology in MDD affecting GM vessels with sizes as large as or larger than arterioles. Pathology in these vessels has not been specifically investigated using MRI and histopathological techniques. However, the general trend for changes observed in the present study and MRI studies points in the same direction: blood vessels exhibit microscopic pathology that is detectable in elderly subjects with depression. Since arterioles and medium-sized vessels are surrounded by smooth muscle it is possible that depression-related neurophysiological changes in vascular innervation brings about microscopic vascular pathology. Arterioles respond to innervation from autonomic ganglia (Sandor, 1999; Hamel, 2006), to perivascular axons from subcortical centers (Hamel, 2006), and to the influence of factors linked to the activity of local neurons and glial cells (Attwell et al., 2010; Anderson and Nedergaard, 2003). In depression, there is evidence for abnormal local neuronal and glial metabolism and functional and neurochemical disturbances (Hamel, 2006; Drevets et al.,

2008; Ordway et al., 2011; Stockmeier et al., 1998) in subcortical sources (locus coeruleus, raphe nuclei, nucleus basalis) innervating arterioles. Thus, future research should clarify the nature of the causal relationship between changes in vessel morphology, local neuronal/glial physiology and cerebrovascular innervation that may account for vascular changes observed in depression.

Increased density of particular size classes of vessel segments and greater perivascular widening in the OFC WM in MDD is consistent with increased density of hyperintensities in deep frontal WM, including OFC WM, revealed by neuroimaging (Taylor et al., 2003a; Greenwald et al., 1998; Herrmann et al., 2008). Increased visibility of perivascular spaces in WM of subjects with MDD may be related to the presence of enhanced Virchow-Robin spaces (Munoz et al., 1993), possibly linked to hyperintensities. However, lacking ante-mortem neuroimaging information, it was not possible to examine a link between vascular changes observed in postmortem tissue and the occurrence of MRI hyperintensities, or how these hyperintensities might be related to perivascular spaces.

Another potential limitation of the present study is that being based on postmortem diagnosis it logically lacked data from standardized antemortem diagnosis. However, there is a high degree of agreement between diagnoses based on next-of-kin and diagnosis based on examination of living subjects (Dejong and Overholser, 2009). This comparison strongly supports the use of retrospective, informant-based interviews to make diagnosis of MDD. In the present study the SCID was used in the interviews with next-of-kin of all subjects (those later deemed MDD subjects as well as those deemed non-psychiatric controls) so that a standardized assessment could be obtained.

The present study failed to demonstrate differences in overall blood vessel density or size between subgroups with early or late-onset MDD. If confirmed, this observation would support the suggestion that disease of small blood vessel as defined by the relatively simple morphological methods used in this research, is not a distinctive feature of MDD even late in life (Thomas et al., 2001). However, it is still possible that molecular changes in blood vessels morphometrically undetectable may distinguish subjects with depression, as has been proposed for the expression of the inflammatory marker ICAM-1 (Thomas et al., 2002a; Thomas et al., 2000).

Supplementary Material

Refer to Web version on PubMed Central for supplementary material.

Acknowledgments

source of funding: Supported by NIH grants: RR017701, MH67996 and MH54846.

We acknowledge the invaluable contributions made by the families consenting to donate brain tissue and be interviewed. We are grateful for the excellent assistance of the Cuyahoga County Coroner's Office in Cleveland, OH. We also thank Herbert Y Meltzer, M.D., and Bryan Roth, M.D., Ph.D., for their assistance in establishing psychiatric diagnoses and Ginny Dilley for assistance in collecting information on the subjects.

References

Alexopoulos GS. The vascular depression hypothesis: 10 years later. Biol Psychiatry. 2006; 60:1304–5. [PubMed: 17157096]

Alexopoulos GS, Meyers BS, Young RC, Kakuma T, Silbersweig D, Charlson M. Clinically defined vascular depression. Am J Psychiatry. 1997; 154:562–5. [PubMed: 9090349]

Anderson CM, Nedergaard M. Astrocyte-mediated control of cerebral microcirculation. Trend Neurosci. 2003; 26:340–4. author reply 344–5. [PubMed: 12850427]

American Psychiatric Association. Diagnostic and Statistical Manual of Mental Disorders. Washington, D.C: American Psychiatric Association; 1994.

Attwell D, Buchan AM, Charpak S, Lauritzen M, Macvicar BA, Newman EA. Glial and neuronal control of brain blood flow. Nature. 2010; 468:232–43. [PubMed: 21068832]

Brassen S, Kalisch R, Weber-Fahr W, Braus DF, Buchel C. Ventromedial prefrontal cortex processing during emotional evaluation in late-life depression: a longitudinal functional magnetic resonance imaging study. Biol Psychiatry. 2008; 64:349–55. [PubMed: 18440493]

Camus V, Kraehenbuhl H, Preisig M, Bula CJ, Waeber G. Geriatric depression and vascular diseases: what are the links? J Affect Disord. 2004; 81:1–16. [PubMed: 15183594]

Coffey CE, Figiel GS, Djang WT, Saunders WB, Weiner RD. White matter hyperintensity on magnetic resonance imaging: clinical and neuroanatomic correlates in the depressed elderly. J Neuropsychiatry Clin Neurosci. 1989; 1:135–44. [PubMed: 2521054]

Coffey CE, Figiel GS, Djang WT, Weiner RD. Subcortical hyperintensity on magnetic resonance imaging: a comparison of normal and depressed elderly subjects. Am J Psychiatry. 1990; 147:187–9. [PubMed: 2301657]

Dejong TM, Overholser JC. Assessment of depression and suicidal actions: agreement between suicide attempters and informant reports. Suicide Life Threat Behav. 2009; 39:38–46. [PubMed: 19298149]

Drevets WC, Price JL, Furey ML. Brain structural and functional abnormalities in mood disorders: implications for neurocircuitry models of depression. Brain Struct Funct. 2008; 213:93–118. [PubMed: 18704495]

Erickson K, Drevets WC, Clark L, Cannon DM, Bain EE, Zarate CA Jr, Charney DS, Sahakian BJ. Mood-congruent bias in affective go/no-go performance of unmedicated patients with major depressive disorder. Am J Psychiatry. 2005; 162:2171–3. [PubMed: 16263859]

Figiel GS, Krishnan KR, Doraiswamy PM, Rao VP, Nemeroff CB, Boyko OB. Subcortical hyperintensities on brain magnetic resonance imaging: a comparison between late age onset and early onset elderly depressed subjects. Neurobiol Aging. 1991; 12:245–7. [PubMed: 1876230]

Grafman J, Schwab K, Warden D, Pridgen A, Brown HR, Salazar AM. Frontal lobe injuries, violence, and aggression: a report of the Vietnam Head Injury Study. Neurology. 1996; 46:1231–8. [PubMed: 8628458]

Greenwald B, Kramer-Ginsberg E, Krishnan K, Ashtari M, Auerbach C, Patel M. Neuroanatomic localization of magnetic resonance imaging signal hyperintensities in geriatric depression. Stroke. 1998; 29:613–7. [PubMed: 9506601]

Hamel E. Perivascular nerves and the regulation of cerebrovascular tone. J Appl Physiol. 2006; 100:1059–64. [PubMed: 16467392]

Herrmann LL, Le Masurier M, Ebmeier KP. White matter hyperintensities in late life depression: a systematic review. J Neurol Neurosug Psychiatry. 2008; 79:619–624.

Krishnan KR, Goli V, Ellinwood EH, France RD, Blazer DG, Nemeroff CB. Leukoencephalopathy in patients diagnosed as major depressive. Biol Psychiatry. 1988; 23:519–22. [PubMed: 3345325]

Krishnan KR, Taylor WD, Mcquoid DR, Macfall JR, Payne ME, Provenzale JM, Steffens DC. Clinical characteristics of magnetic resonance imaging-defined subcortical ischemic depression. Biol Psychiatry. 2004; 55:390–7. [PubMed: 14960292]

Krishnan KRR. Depression as a contributing factor in cerebrovascular disease. Am Heart J. 2000; 140:S70–S76.

Kumar A, Miller D. Neuroimaging in late-life mood disorders. Clin Neurosci. 1997; 4:8–15. [PubMed: 9056117]

Lai T, Payne ME, Byrum CE, Steffens DC, Krishnan KR. Reduction of orbital frontal cortex volume in geriatric depression. Biol Psychiatry. 2000; 48:971–5. [PubMed: 11082470]

Lee SH, Payne ME, Steffens DC, Mcquoid DR, Lai TJ, Provenzale JM, Krishnan KR. Subcortical lesion severity and orbitofrontal cortex volume in geriatric depression. Biol Psychiatry. 2003; 54:529–33. [PubMed: 12946881]

Lesperance F, Frasure-Smith N, Theroux P, Irwin M. The association between major depression and levels of soluble intercellular adhesion molecule 1, interleukin-6, and C-reactive protein in patients with recent acute coronary syndromes. Am J Psychiatry. 2004; 161:271–7. [PubMed: 14754776]

Lesser IM, Mena I, Boone KB, Miller BL, Mehringer CM, Wohl M. Reduction of cerebral blood flow in older depressed patients. Arch Gen Psychiatry. 1994; 51:677–86. [PubMed: 8080344]

Macfall JR, Payne ME, Provenzale JE, Krishnan KR. Medial orbital frontal lesions in late-onset depression. Biol Psychiatry. 2001; 49:803–6. [PubMed: 11331089]

Miguel-Hidalgo JJ, Rajkowska G. Immunohistochemistry of neural markers for the study of the laminar architecture in celloidin sections from the human cerebral cortex. J Neurosci Meth. 1999; 93:69–79.

Munoz DG, Hastak SM, Harper B, Lee D, Hachinski VC. Pathologic correlates of increased signals of the centrum ovale on magnetic resonance imaging. Arch Neurol. 1993; 50:492–7. [PubMed: 8489405]

Ordway GA, Szebeni A, Chandley MJ, Stockmeier CA, Xiang L, Newton SS, Turecki G, Duffourc MM, Zhu MY, Zhu H, Szebeni K. Low gene expression of bone morphogenetic protein 7 in brainstem astrocytes in major depression. Int J Neuropsychopharmacol. 2011; 15:855–868. [PubMed: 21896235]

Rajkowska G, Goldman-Rakic PS. Cytoarchitectonic definition of prefrontal areas in the normal human cortex: I. quantitative criteria for distinguishing areas 9 and 46. Cereb Cortex. 1995; 4:307–322. [PubMed: 7580124]

Rajkowska G, Miguel-Hidalgo JJ, Dubey P, Stockmeier CA, Krishnan KRR. Prominent reduction in pyramidal neurons density in the orbitofrontal cortex of elderly depressed patients. Biol Psychiatry. 2005; 58:297–306. [PubMed: 15953590]

Rajkowska G, Miguel-Hidalgo JJ, Wei J, Dilley G, Pittman SD, Meltzer HY, Overholser JC, Roth BL, Stockmeier CA. Morphometric evidence for neuronal and glial prefrontal cell pathology in major depression. Biol Psychiatry. 1999; 45:1085–98. [PubMed: 10331101]

Sandor P. Nervous control of the cerebrovascular system: doubts and facts. Neurochem Int. 1999; 35:237–59. [PubMed: 10458655]

Savitz J, Van Der Merwe L, Solms M, Ramesar R. Neurocognitive function in an extended Afrikaner-ancestry family with affective illness. J Psychiatry Neurosci. 2007; 32:116–20. [PubMed: 17353940]

Steffens D, Krishnan K. Structural neuroimaging and mood disorders: recent findings, implications for classification, and future directions. Biol Psychiatry. 1998; 43:705–12. [PubMed: 9606523]

Steffens DC, Helms MJ, Krishnan KR, Burke GL. Cerebrovascular disease and depression symptoms in the cardiovascular health study. Stroke. 1999; 30:2159–66. [PubMed: 10512922]

Stockmeier CA, Shapiro LA, Dilley GE, Kolli TN, Friedman L, Rajkowska G. Increase in serotonin-1A autoreceptors in the midbrain of suicide victims with major depression-postmortem evidence for decreased serotonin activity. J Neurosci. 1998; 18:7394–401. [PubMed: 9736659]

Taylor, WD.; Krishnan, RR. Affective Disorders: Imaging Studies. In: SOARES, JC.; GERSHON, S., editors. Handbook of medical psychiatry. New York: Marcel Dekker, Inc; 2003.

Taylor WD, Macfall JR, Steffens DC, Payne ME, Provenzale JM, Krishnan KR. Localization of age-associated white matter hyperintensities in late-life depression. Prog Neuropsychopharmacol Biol Psychiatry. 2003a; 27:539–44. [PubMed: 12691791]

Taylor WD, Payne ME, Krishnan KR, Wagner HR, Provenzale JM, Steffens DC, Macfall JR. Evidence of white matter tract disruption in MRI hyperintensities. Biol Psychiatry. 2001; 50:179–83. [PubMed: 11513816]

Taylor WD, Steffens DC, Macfall JR, Mcquoid DR, Payne ME, Provenzale JM, Krishnan KRR. White Matter Hyperintensity Progression and Late-Life Depression Outcomes. Arch Gen Psychiatry. 2003b; 60:1090–1096. [PubMed: 14609884]

Thomas AJ, Ferrier IN, Kalaria RN, Davis S, O'brien JT. Cell adhesion molecule expression in the dorsolateral prefrontal cortex and anterior cingulate cortex in major depression in the elderly. Br J Psychiatry. 2002a; 181:129–34. [PubMed: 12151283]

Thomas AJ, Ferrier IN, Kalaria RN, Perry RH, Brown A, O'brien JT. A neuropathological study of vascular factors in late-life depression. J Neurol Neurosurg Psychiatry. 2001; 70:83–87. [PubMed: 11118253]

Thomas AJ, Ferrier IN, Kalaria RN, Woodward SA, Ballard C, Oakley A, Perry RH, O'brien JT. Elevation in late-life depression of intercellular adhesion molecule-1 expression in the dorsolateral prefrontal cortex. Am J Psychiatry. 2000; 157:1682–4. [PubMed: 11007725]

Thomas AJ, O'brien JT, Barber R, Mcmeekin W, Perry R. A neuropathological study of periventricular white matter hyperintensities in major depression. J Affect Disord. 2003; 76:49–54. [PubMed: 12943933]

Thomas AJ, O'brien JT, Davis S, Ballard C, Barber R, Kalaria RN, Perry RH. Ischemic basis for deep white matter hyperintensities in major depression: a neuropathological study. Arch Gen Psychiatry. 2002b; 59:785–92. [PubMed: 12215077]

Uylings HB, Sanz-Arigita EJ, De Vos K, Pool CW, Evers P, Rajkowska G. 3-D cytoarchitectonic parcellation of human orbitofrontal cortex correlation with postmortem MRI. Psychiatry Res. 2010; 183:1–20. [PubMed: 20538437]

Vaishnavi S, Taylor WD. Neuroimaging in late-life depression. Int Rev Psychiatry. 2006; 18:443–51. [PubMed: 17085363]

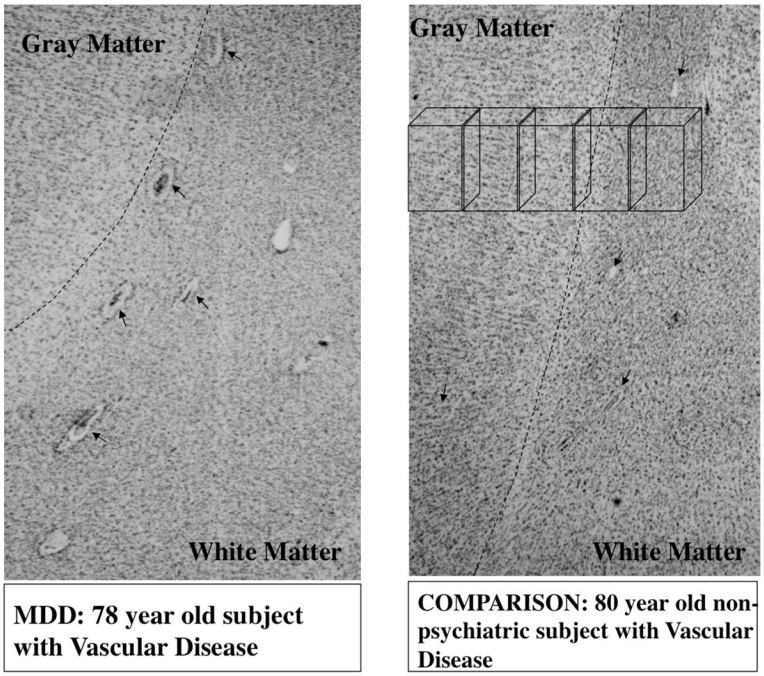

Figure 1.

Micrographs at low power of Nissl stained sections from a subject with major depression (left panel) and non-psychiatric comparison subject (right panel). Arrows point to blood vessels visible in both micrographs in gray and white matter. Note the wider non-stained spaces between blood vessels and the brain parenchyma in the subject with depression. Broken lines signal the border between gray and white matter. A series of boxes in the top portion of right panel represents the sampling frames within which blood vessels segments were measured.

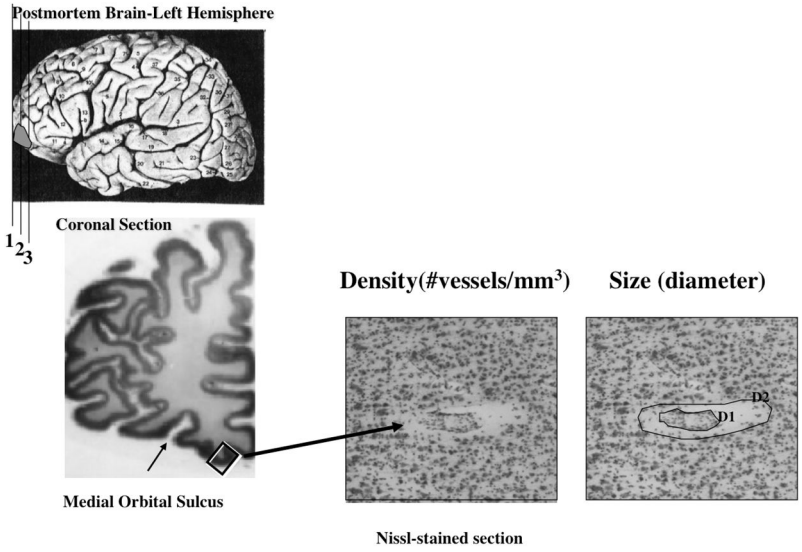

Figure 2.
Location in the left cerebral hemisphere of the cortical area examined in the present study (left panels). Higher power micrographs of one Nissl-stained vessel fragment denoting the perimeter of the segment itself (D1) and the perimeter lining the space between the vessel and the brain parenchyma (D2).

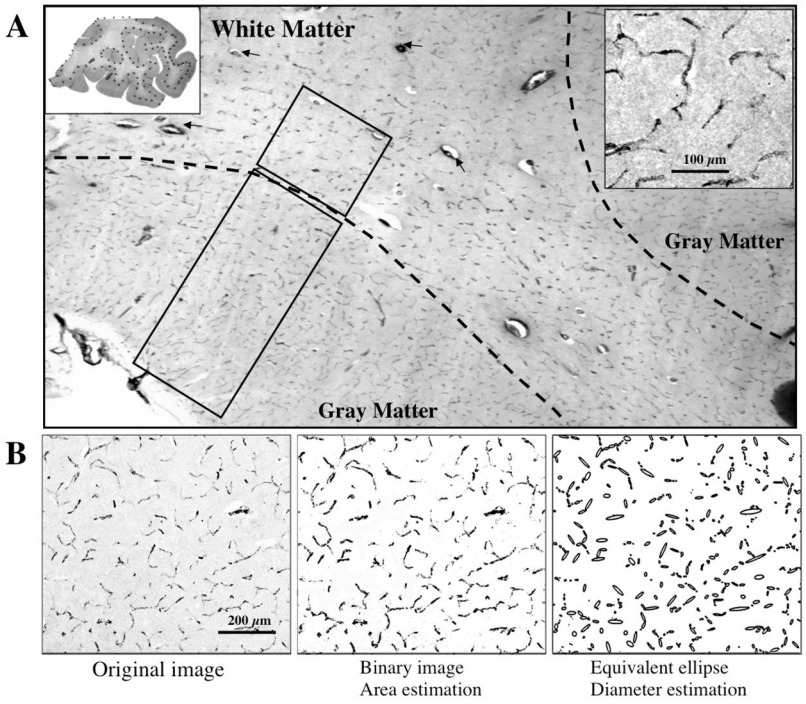

Figure 3.

Blood vessels immunoreactive for von Willebrand Factor (vWF) in the human orbitofrontal cortex. A) vWF positive vessels are present in both gray and white matter. Rectangles in gray and white matter depict the sample frames where measurements of vessel segments were performed. The top left inset shows a whole section processed for vWF immunohistochemistry. The Dotted line separates gray from white matter. The top right inset shows a high magnification picture of vWF-IR vessel profiles in the gray matter. B) The left panel shows a gray-level micrograph of vWF-immunoreactive vessel segments; the middle panel is a binary image of the left panel, and is used to calculate the area fraction occupied by vessels segments in the 2-dimensional micrograph. The right panel presents the equivalent ellipses generated in the ImageJ software for each of the continuous vessel profiles in the other panels, the minor axes of those ellipses were used for an estimation of the vessel diameter in immunoreactive preparations.

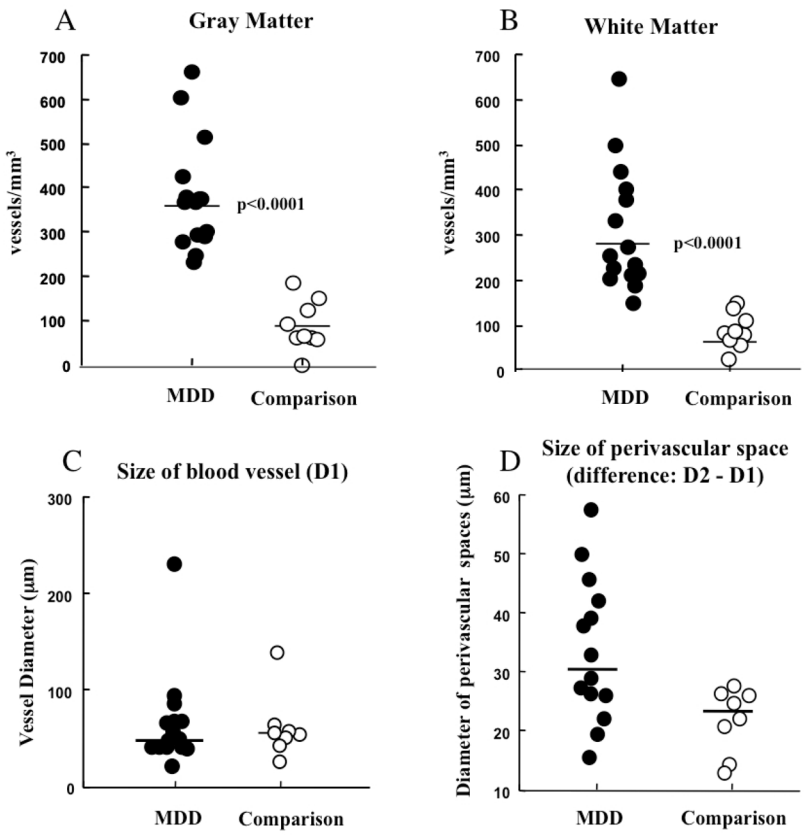

Figure 4.

Graphs representing values of density (A, B) and size (C,D) of Nissl-stained vessels segments in subjects with major depressive disorder (MDD) and non-psychiatric comparison subjects (Comparison). A) Density in the gray matter. B) Density in the white matter. C) Average diameter. D) Differential diameter of the perivascular space (see figure 2). Horizontal bars represent the median.

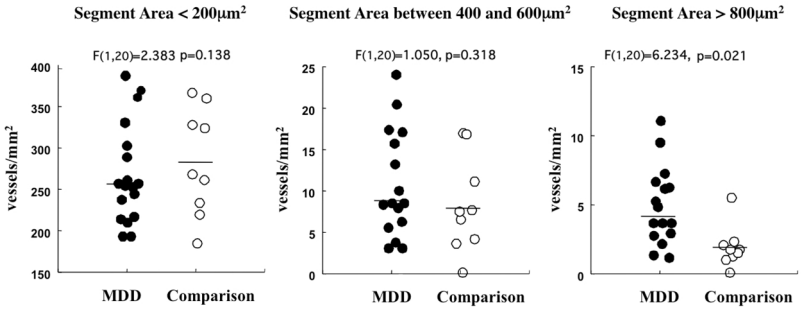

Figure 5.

Density of vWF immunoreactive vessel segments of different 2-dimensional sizes (<200 μm^2, between 400 and 600 μm^2, >800 μm^2). Only vessel segments with sizes over 800 μm^2 had significantly higher densities in MDD subjects than in non-psychiatric comparison subjects. Horizontal bars represent the median.

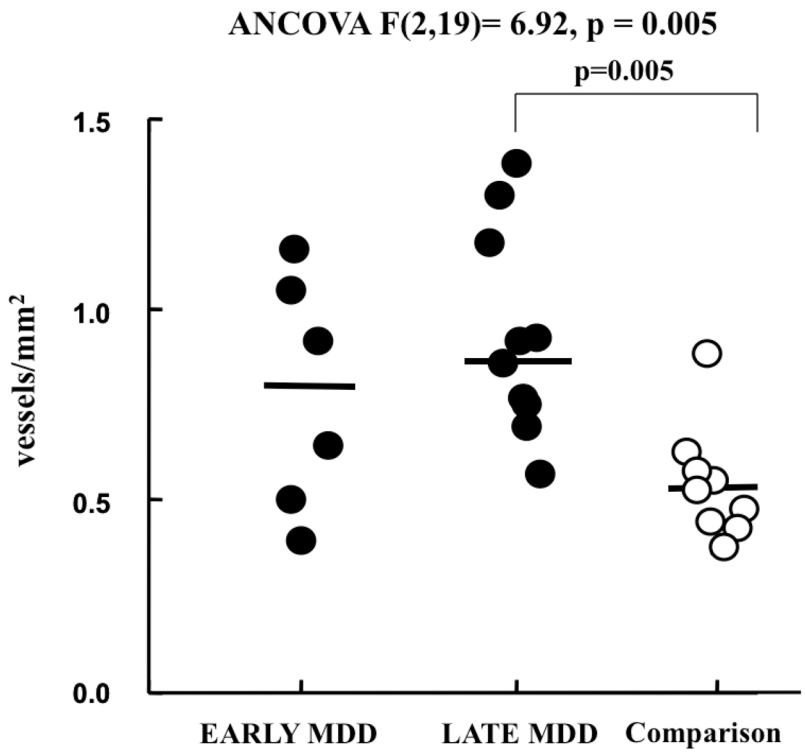

Figure 6.

Graph representing individual values for the density of vessels larger than 60 mm^2 and having perivascular spaces in subjects with early onset MDD, late onset MDD and non-psychiatric comparison subjects. The density of those vWF segments in white matter was significantly higher in late onset MDD subjects than in comparison subjects, but it was not significantly different in early onset MDD subjects. Horizontal bars represent the median.

Table 1

#	Diagnosis /VsD	Age/ gender	PMI (hr)	TF	Cause of Death	Psychotropic medication	Drugs/ Alcohol History	Toxicology[a]	Family History	MDD Onset (age)	Dur MDD yrs.	Responder/ Nonresponder
1	MDD/VsD+	86/M	21	5.6	S/stabbing	fluoxetine*	none	none detected	suicide	55	30	nonresponder
2	MDD/VsD+	81/M	33	28.5	S/drowning	sertraline*	none	none detected	AA, SA depression	81	0.17	N/A
3	MDD/VsD+	82/M	12	60.3	S/CO poisoning	sertraline* risperdal*	none	CO		22	60	nonresponder
4	MDD/VsD+/−	73/M	10	15.9	S/hanging	nortriptyline*	none	nortriptyline, etoh	none	66	7	responder
5	MDD/VsD+/−	78/F	25	6.4	S/jumping	lorazepam	none	none detected	none	73	5	N/A
6	MDD/VsD+/−	72/F	19	46	S/drowning	trazodone*, lorazepam*, temazepam*	none	norpropoxyphene propoxyphene	none	72	0.75	nonresponder
7	MDD/No VsD	78/M	26.5	19	S/hanging	sertaline*	none	sertraline, pos norsertraline	none	78	0.2	nonresponder
8	MDD/No VsD	74/M	25	17	S/SIGSW Head	chlorpromazine trazodone clorazepate methylphenidate	AA, SA	diazepam acetaminophen	AA	50	24	N/A
9	MDD/rem/VsD+	72/F	17	15.1	N/CVD (heart attack)	fluoxetine	none	none detected	none	69	3	noncompliant
10	MDD/VsD+	73/F	17	25.1	N/aortic aneurism	lithium nortriptyline* restoril clonazepam*	AD for 40 years stopped 8 years before death	none detected	AA, anxiety, depression	23	50	N/A
11	MDD/VsD+	78/M	26	10.7	N/severe coronary heart disease	sertraline*, clonazepam*, carbamezapine*, amoxapine, imipramine, chlordiazepoxide, benztropine, nortriptyline, fluoxetine, temazepam, haloperidol, trazodone, loxipine, lithium	AA	carbamezepine, chlorpheniramine pos, sertraline	depression, AA, anxiety	56	22	responder
12	MDD/VsD+/−	87/F	24	42.9	N/aortic aneurism due to heart disease	trazodone flurazepam*	none	diphenyhydramine	none	67	20	N/A
13	MDD/VsD+/−	62/M	17	23.5	N/bronchopneumonia due to coronary sclerotic heart disease	diazepam*	AD, SA	ethanol, diazepam, diazapin	depression, SA	32	30	N/A
14	MDD/INS/VsD	67/F	17	13.8	N/rupture of atherosclerothoracic aorta	alprazolam, doxepin*	none	none detected	anxiety, AA	37	30	responder
15	MDD/INS/VsD	63/F	24	11.9	N/pulmonary thromboembolism	chlorpromazine*, clonazepam* amitriptyline*, amantadine*	SA (20 years) AA (25 years)	amitriptyline, chlorpromazine amantadine nortriptyline lidocaine	AA, anxiety	33	30	nonresponder
16	MDD/No VsD	54/M	23	12	S/CO poisoning	sertraline*	none	CO, phenobarbital, phenytoin	AA	51	3	N/A

Int J Geriatr Psychiatry. Author manuscript; available in PMC 2014 September 01.

#	Diagnosis /VsD	Age/ gender	PMI (hr)	TF	Cause of Death	Psychotropic medication	Drugs/ Alcohol History	Toxicology[a]	Family History	MDD Onset (age)	Dur MDD yrs.	Responder/ Nonresponder
Avg		74	21	22.1								
17	CTRL/INS/VsD	71/M	24	21.8	N/cardiac rupture	none	AD for 20 yrs. stopped 32 yrs before death	none detected	AA			
18	CTRL/VsD+	58/M	21.5	34.4	N/heart disease	none	none	none detected	AA, SA			
19	CTRL/INS/VsD	69/M	18	36.1	N/dissecting aortic aneurism	none	none	none detected	AA, depression			
20	CTRL/VsD+	77/M	24	30.2	N/heart disease	none	none	none detected	SA			
21	CTRL/VsD+	70/M	20	12.7	N/heart complications	clonazepam (for leg twitch)	AA stopped 30 yrs before death	none detected	AA			
22	CTRL/VsD+	80/F	21	25.6	N/hypertensive coronary sclerotic heart disease w/ remote myocardial infarct	none	none	none detected	AD			
23	CTRL/VsD+	86/F	18	18.7	N/coronary sclerotic heart disease with myocardial fibrosis and cardiomegaly	none	none	diltiazem	none			
24	CTRL/VsD+	67/M	24	32.6	N/atherosclerotic cardiovascular disease	none	none	none detected	AA, depression			
25	CTRL/VsD+/−	60/F	19	10.2	N/aortic aneurism	none	none	none detected	N/A			
Avg		71	21	24.7								

AA- Alcohol abuse; AD- Alcohol Dependence; Avg- average; CTRL- control; F- female; INS/VsD – insufficient data to make a VsD diagnosis; M- male; MDD- major depressive disorder; N – natural causes; N/A-not available; PMI- postmortem interval (hours) defined as the time between death and the beginning of formalin fixation; rem- recurrent MDD, in remission; S- Suicide; SA- Substance Abuse; SIGSW- single gunshot wound; TF- time in formalin; VsD - vascular disease; VsD+ - strong VsD; VsD+/− - moderate VsD.

[*] Drugs which were prescribed in last month of life.

[a] Present in toxicology screen of blood.

Int J Geriatr Psychiatry. Author manuscript; available in PMC 2014 September 01.